Research Article

Ultrasound Assisted Synthesis of Tryptanthrins Catalyzed By Zinc Oxide Nanoparticles

Sonatai Patil[1], Ananda Mane[2], Savita Dhongade-Desai[1]*

[1]Research Laboratory in Heterocyclic Chemistry, Devchand College Arjunnagar, Kolhapur, 591269, M.S., India
[2]Department of Chemistry, KIT's College of Engineering, Kolhapur, 416234, M.S., India

Abstract

We have explored the catalytic potential of ZnO nanoparticles for efficient synthesis of tryptanthrins through the reaction of isatoic anhydrides and isatins under ultrasonic irradiation. The present method is of great interest due to its salient features such as short reaction time, simple work-up, excellent yield of products, high functional group tolerance and environment compatibility. The synergetic effect of ZnO nanoparticles and ultrasound irradiation has been discussed. Notably, the nanocatalyst could be recovered and reused for four times without noticeable decrease in the catalytic activity.

Keywords: Heterogeneous catalysis, Zinc Oxide nanoparticles, Trypthanthrin, Ultrasonication

***Correspondence**

Author: Savita Dhongade-Desai
Email: savitadesai2010@gmail.com

Introduction

Tryptanthrin is a natural alkaloid characterized by a novel indolo[2,1-*b*]quinazoline ring system. It is acknowledged as a potent therapeutic agent and obtained from various natural plant sources [1–2]. Tryptanthrin is considered as a biogenetic precursor for designing potential drugs with diverse medical functions including anticancer, antiprotozoal, antiparasitic, antineoplastic and antileishmanial properties [3]. In addition, antioxidant [4], antimicrobial [5] and antitubercular [6] activities of tryptanthrin have also been reported. Its effective use against allergy [7], intestinal disorders [8] and inflammatory bowel disorders [9] has been very well demonstrated. More importantly, the physicochemical properties of tryptanthrin derivatives and usefulness of tryptanthrin compounds as pigments, dyes and photoelectric materials have also been investigated [10–11].

In the light of intriguing bioactivities, different methodologies have been developed for the synthesis of tryptanthrin and its derivatives. The most studied synthetic approach to indolo[2,1-*b*]quinazoline core focuses on the use of isatin through the reaction of isatin with isatoic anhydride in presence of β-cyclodextrin [12] and cobalt(III)–porphyrin complex (CoTCPP) as a catalyst [13], treatment of isatin with $POCl_3$ [14], cathodic reduction of isatin [15], coupling of *ortho*-aminobenzoic acid with isatin using $SOCl_2$ [16], tert-butyl hydroperoxide/K_3PO_4 promoted oxidative cyclization of isatins [17] and palladium(0)/chiral ligand-catalyzed asymmetric decarboxylative cyclization of vinyl benzoxazinanones with isatins [18]. Oxidative dimerization of isatin or indole including oxidation of isatin with $KMnO_4$ [19], copper catalyzed oxidation of indole [20], Dakin oxidation of indole-3-carbaldehyde [21] and oxone induced oxidation of indole-3-carbaldehyde [22] also led to the formation of tryptanthrin. In addition, the reaction of 2-bromophenyl isocyanide with electrophilic methyl-2-isocyanatobenzoate [23], I_2-tert-butyl hydro peroxide catalyzed intramolecular amination [24], insertion of aryne intermediate to quinazolinones [25], copper catalyzed reactions [26–27] and visible light mediated photoredox catalysis [28–30] have been developed for the synthesis of tryptanthrin. Unfortunately, some of these reported transformations are not environment friendly and

suffer from one or more limitations such as high reaction temperature, lower yield of the desired product, toxicity and recovery and recyclability of the catalyst. Therefore the development of new synthetic protocols involving use of low cost, readily available and reusable catalyst with high catalytic activity for the synthesis of tryptanthrins is strongly desirable.

Now a day's catalysis by metal oxide nanoparticles has attracted considerable attention under the heading of "green chemistry" because of their significant properties such as high chemical activity, environmental compatibility, operational simplicity and reusability. Among the various metal oxide nanocatalysts, zinc oxide (ZnO) is a renowned catalyst due to the presence of both Lewis acidic (Zn^{2+}) and Lewis basic (O^{2-}) sites on surface. Different morphologies and range of particle sizes for ZnO NPs led to diverse investigations in industrial and academic societies [31–33]. In addition, it has been employed as an efficient heterogeneous catalyst in various organic transformations [34–37]. Ultrasonication, based on cavitation effects leading to mass transfer improvement is an innocuous technique in organic synthesis. The notable features of the ultrasound are enhanced reaction rates, formation of purer products with higher yields, increased selectivity, easier manipulation and low energy conservation. These advantages have motivated the organic chemists to explore the applications of ultrasound in heterogeneous catalysis for the synthesis of diverse bioactive molecules [38–41].

In agreement with abovementioned importance of ZnO NPs and bioactivities of tryptanthrin derivatives, herein we wish to explore the catalytic potential of ZnO NPs for the synthesis of indolo[2,1-*b*]quinazoline-6,12-diones under ultrasonication.

Experimental

Chemicals and Apparatus

All the chemicals were obtained from Merk Company and used as received. The melting points of products were measured in open capillary tubes and are uncorrected. Infrared spectra were recorded on Perkin Elmer FT-IR spectrometer. ^{1}H and ^{13}CNMR spectra were recorded on a Brucker-Avance 300 MHz spectrometer using TMS as an internal standard and $CDCl_3$/DMSO-d_6 as a solvent. Mass spectra were recorded on Shimadzu QP 2010 GCMS. The X-ray diffraction (XRD) measurements of the catalyst powder were recorded by a Phillips diffractometer of X'pert company with monochromatized Cu Kα radiation (λ =1.5406 Å). Microscopic morphology of nanocatalyst was visualized by scanning electron microscopy (SEM) (LEO 1455VP). Sonication was performed in SPECTRALAB-UCB-30 ultrasonic bath with a frequency of 30 kHz and the output power of 100 W through manual adjustment. The ultrasonic apparatus showed the temperature automatically so the temperature of reaction medium was controlled and fixed at room temperature by water circulator in case of any elevation in temperature.

Synthesis of ZnO nanoparticles

ZnO nanoparticles were synthesized according to the previously reported method [42]. To the aqueous solution (0.5 M) of zinc nitrate hexahydrate, aqueous potassium hydroxide solution (0.9 M) was added dropwise at room temperature under vigorous stirring. The obtained white precipitate of zinc hydroxide was then centrifuged at 5000 rpm for 20 min and consequently washed with deionized water and absolute ethanol. The resultant precipitate was eventually calcined at 400 °C for 24 h in the furnace without any special atmosphere to produce ZnO nanoparticles under thermal decomposition condition.

General procedure for the synthesis of tryptanthrin

A mixture of isatin (1 mmol), isatoic anhydride (1 mmol) and ZnO nanoparticles (8 mg, 10 mol%) in THF (5 mL) was irradiated by ultrasound at room temperature for required reaction time as indicated in **Table 1**. The progress of the reaction was monitored by thin layer chromatography by using petroleum ether: ethyl acetate (7:3) as solvent system. After completion of the reaction to separate the catalyst from the product, the solid product was dissolved in ethyl acetate and nanoparticles of catalyst were separated by centrifugation. The residue obtained after solvent evaporation was purified by column chromatography to afford pure indolo[2,1-*b*]quinazoline-6,12-dione.

Spectral data of representative compounds

Indolo[2,1-b]quinazoline-6,12-dione (3a)

Yellow solid; m.p. 272 °C. ^{1}H NMR (300 MHz, $CDCl_3$): δ 8.65 (d, *J* = 8.1 Hz, 1H), 8.46 (d, *J* = 6.6 Hz, 1H), 8.06 (dd, *J* = 8.1 Hz, *J* = 0.6 Hz, 1H), 7.94 (dd, *J* = 7.8 Hz, *J* = 0.9 Hz, 1H), 7.90–7.84 (m, 1H), 7.83–7.78 (m, 1H), 7.72–

7.67 (m, 1H), 7.47–7.42 (m, 1H) ppm. ^{13}C NMR (75 MHz, $CDCl_3$): δ 182.5, 158.1, 146.6, 146.3, 138.2, 135.1, 130.7, 130.2, 127.5, 127.1, 125.4, 123.7, 121.9, 117.9 ppm. MS (EI): calcd for $C_{15}H_8N_2O_2$: 248; found: 248 (M^+).

8-Chloroindolo[2,1-b]quinazoline-6,12-dione (3d)

Yellow solid; m.p. 294 °C. ^{1}H NMR (300 MHz, $CDCl_3$): δ 8.62 (d, *J* = 8.7 Hz, 1H), 8.46 (dd, *J* = 7.8 Hz, J = 1.2 Hz, 1H), 8.06 (d, *J* = 7.2 Hz, 1H), 7.92–7.86 (m, 2H), 7.78–7.69 (m, 2H) ppm. ^{13}C NMR (75 MHz, $CDCl_3$): δ 191.1, 166.1, 160.0, 146.5, 135.2, 130.8, 130.5, 127.5, 124.9, 124.6, 123.7, 119.7, 119.6, 112.2, 111.8 ppm. MS (EI): calcd for $C_{15}H_7ClN_2O_2$: 282; found: 282 (M^+).

8-Bromoindolo[2,1-b]quinazoline-6,12-dione (3e)

Brown solid; m.p. 292 °C. ^{1}H NMR (300 MHz, DMSO): δ 8.39 (d, *J* = 9.3 Hz, 1H), 8.31 (d, *J* = 7.8 Hz, 1H), 8.03 (dd, *J* = 6.9 Hz, *J* = 2.1 Hz, 2H), 7.95 (d, *J* = 3.6 Hz, 2H), 7.77–7.72 (m, 1H) ppm. ^{13}C NMR (75 MHz, DMSO): δ 181.7, 158.9, 145.9, 144.3, 140.2, 134.8, 134.1, 130.2, 129.6, 128.2, 127.2, 122.6, 122.4, 120.6, 119.4 ppm. MS (EI): calcd for $C_{15}H_7BrN_2O_2$: 325; found: 328 (M^+).

8-Fluoroindolo[2,1-b]quinazoline-6,12-dione (3f)

Yellow solid; m.p. 262 °C. ^{1}H NMR (300 MHz, $CDCl_3$): δ 8.66 (dd, *J* = 9.0 Hz, *J* = 4.2 Hz, 1H), 8.46 (d, *J* = 7.8 Hz, 1H), 8.06 (d, *J* = 8.1 Hz, 1H), 7.88 (t, *J* = 7.8 Hz, 1H), 7.71 (t, *J* = 7.5 Hz, 1H), 7.60 (dd, *J* = 6.3 Hz, *J* = 2.4 Hz, 1H), 7.54–7.47 (m, 1H) ppm. ^{13}C NMR (75 MHz, $CDCl_3$): δ 200.9, 181.8, 175.9, 173.3, 169.8, 162.0, 150.5, 138.2, 135.6, 133.6, 130.9, 127.6, 119.2 ppm. MS (EI): calcd for $C_{15}H_7FN_2O_2$: 266; found: 266 (M^+).

Results and Discussion

The microstructures of the synthesized ZnO nanoparticles were confirmed by X-ray diffractometer (XRD), energy dispersive X-ray (EDX) and scanning electron microscope (SEM) spectroscopy. The XRD pattern of ZnO nanoparticles is shown in **Figure 1**. The observed diffraction peaks at 2θ values of 31.81, 34.46, 36.28, 47.57, 56.63, 62.89, 66.41, 67.98, 69.12, 72.58 and 77.03 corresponds to (100), (002), (101), (102), (110), (103), (200), (112), (201), (004) and (202) *hkl* planes. The observed d-spacing values for different *hkl* planes are in good agreement with JCPDS card number 36-1451 [43]. The sharp and intense diffraction peaks revealed that the ZnO nanoparticles are polycrystalline in nature with hexagonal (primitive) phase. The average crystallite size of ZnO nanoparticles was estimated using Debye–Scherrer's equation (D=$K\lambda/\beta\cos\theta$) [44] and found to be 25.86 nm.

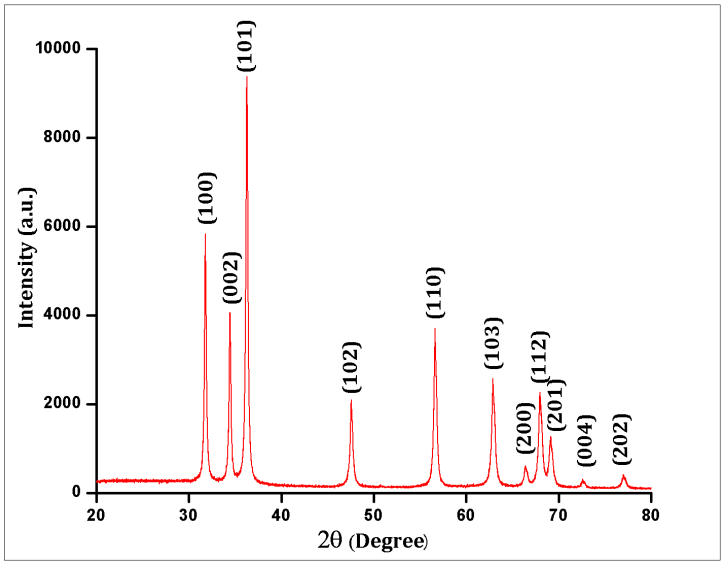

Figure 1 The XRD pattern of ZnO nanoparticles

The chemical composition of the prepared ZnO nanoparticles as well as its stoichiometry was determined by EDX studies. The EDX spectrum of ZnO NPs is shown in **Figure 2**, which indicates the presence of zinc and oxygen as the only elementary components. The SEM image of ZnO nanoparticles is shown in **Figure 3**. Which clearly indicate that the average diameter of ZnO nanoparticles is in the range 25 to 30 nm.

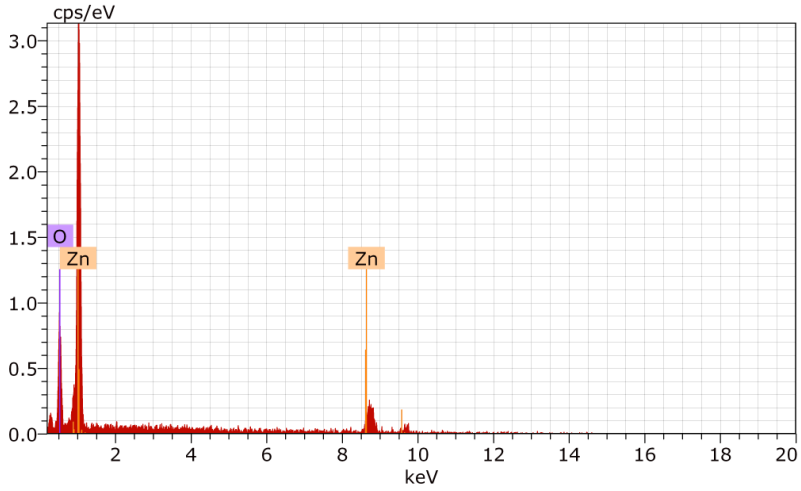

Figure 2 The EDX pattern of ZnO nanoparticles

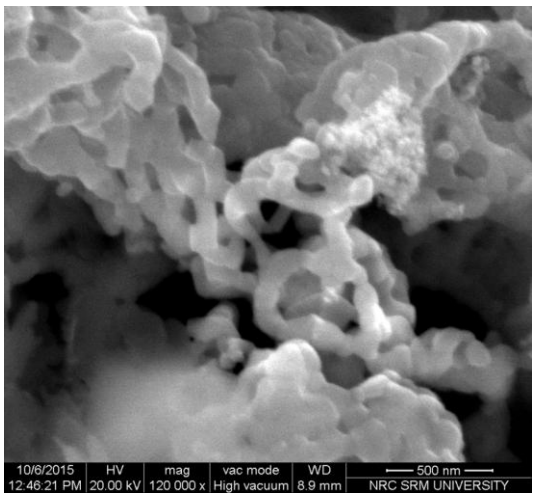

Figure 3 The SEM image of ZnO nanoparticles

Initial experimentation begins with the optimization of reaction parameters for the model reaction between isatoic anhydride (**1a**) and isatin (**2a**) to yield indolo[2,1-*b*]quinazoline-6,12-dione (**3a**) in the presence of ZnO nanoparticles under ultrasonication at room temperature (**Scheme 1**).

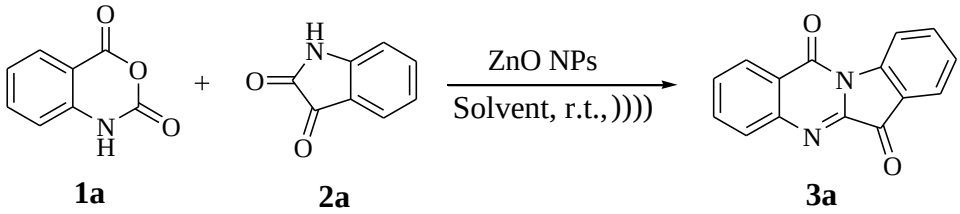

1a **2a** **3a**

Scheme 1 Synthesis of indolo[2,1-*b*]quinazoline-6,12-dione using ZnO nanoparticles under ultrasound irradiation at room temperature.

Initially the model reaction was run in water under stirring for 180 min at room temperature, but no formation of desired product indolo[2,1-*b*]quinazoline-6,12-dione (**3a**) was observed by TLC (Table 1, entry 1). It might be due to the insolubility of substrates in water. Then the model reaction was run in solvents like ethanol, methanol, dichloromethane, acetonitrile and dimethyl formamide at room temperature for 180 min and noticed 30-45% product yield (Table 1, entries 2–6). But relatively better yield (52%) of product **3a** was noticed in tetrahydrofuran within 180 min of stirring at room temperature (Table 1, entry 7). Then we have carried out the model reaction in different solvents under ultrasonic irradiation and in all cases, it was noted that the reaction times are shorter and the yields of the product are higher under sonication. Interestingly, the shortest reaction time and best yield were obtained in tetrahydrofuran under ultrasonication (Table 1, entry 7). In view of these observations we have selected THF as the reaction medium for ZnO nanoparticles catalyzed synthesis of indolo[2,1-*b*]quinazoline-6,12-diones under ultrasonic

irradiation. When the model reaction was performed in THF at room temperature in the absence of catalyst without ultrasonic irradiation, no formation of desired was noticed. Whereas, in the presence of ZnO nanoparticles and in the absence of ultrasonic irradiation, the product was obtained with lower yield and with longer reaction time (Table 1, entry 7). However, in the presence of ultrasonic irradiation and 10 mol % of catalyst, the yield increased to 92 % and reaction time reduced to 30 min (Table 1, entry 7). These observations demonstrated that the synergetic effect of ultrasonication and ZnO nanoparticles played an important role in catalyzing the reaction. In all cases (Table 1, entries 2–7), the result showed that the reaction times are shorter and the yields of the products are higher under ultrasonic condition. The reason may be the phenomenon of cavitation, a physical process that creates, enlarges and implodes gaseous cavities in an irradiated liquid, therefore increasing the mass transfer and allowing chemical reactions to take place.

Next we examined the effect of amount of catalyst on the yield of model reaction. The model reaction was performed in the presence of different amounts of catalyst and results are recorded in **Table 2**. It noted that the maximum yield was obtained with 10 mol % of catalyst and increase in amount of catalyst further to 12 mol % failed to increase the yield.

Table 1 Optimization in the presence of different solvents[a]

Entry	Solvent	Without Ultrasound[b]		With Ultrasound[c]	
		Time[d] (min)	Yield[e] (%)	Time[d] (min)	Yield[e] (%)
1	Water	180	No reaction	45	No reaction
2	Ethanol	180	30	30	65
3	Methanol	180	45	30	72
4	Dichloromethane	180	40	30	70
5	Acetonitrile	180	35	30	58
6	Dimethyl Formamide	180	30	30	65
7	**Tetrahydrofuran**	180	**52**	**30**	**92**

[a]Reaction conditions: isatoic anhydride (1 mmol), isatin (1 mmol), ZnO nanoparticles (catalytic amount) and solvent 5 mL. Reaction temperature 30 °C; [b]Reaction under stirring condition without ultrasound. Reaction temperature 30 °C; [c]Reaction performed under ultrasonication with irradiation frequency 30 kHz and ultrasonic power 100 W at room temperature 30 °C; [d] Reaction progress monitored by TLC; [e]Isolated yield.

Table 2 Effect of amount of ZnO nanoparticles on the yield of indolo[2,1-*b*]quinazoline-6,12-dione[a]

Entry	Amount of catalyst (mol %)	Reaction time[b] (min)	Yield[c]
1	2	30	68
2	4	30	74
3	6	30	80
4	8	30	86
5	**10**	**30**	**92**
6	12	30	92

[a]Reaction conditions: isatoic anhydride (1 mmol), isatin (1 mmol), ZnO nanoparticles and THF 5 mL under sonic condition with irradiation frequency 30 kHz and ultrasonic power 100 W at room temperature 30 °C; [b]Reaction progress monitored by TLC; [c]Isolated yield.

Next, in order to evaluate the effect of irradiation frequency on the product yield of model reaction, we have carried out two experiments respectively at 30 and 40 kHz. When the irradiation frequency was 30 kHz, the yield of **3a** was found to be 92 % (**Table 3**, entry 1). The yield of **3a** (90 %) (Table 3, entry 2) was found to be almost same at 40 kHz. It was noticed that, with increase of irradiation frequency from 30 to 40 kHz, the reaction yield was not affected to a measurable amount. Therefore the synthesis of indolo[2,1-*b*]quinazoline-6,12-diones was carried out at the frequency of 30 kHz at room temperature.

The catalytic efficiency of ZnO nanoparticles for the synthesis of indolo[2,1-*b*]quinazoline-6,12-dione has been compared with bulk ZnO and the results are summarized in **Table 4**. It was noticed that the catalytic activity of ZnO nanoparticles is much better than bulk ZnO. Due to morphological changes the reactivity of ZnO nanoparticles is greatly enhanced compared to bulk ZnO. Larger crystallites of ZnO have a small percentage of reactive sites on the surface whereas; smaller crystallites of ZnO will possess a much higher surface concentration of active sites.

Table 3 Effect of different frequencies of ultrasound irradiation on the synthesis of indolo[2,1-*b*]quinazoline-6,12-dione

Entry	Irradiation frequency (Hz)	Reaction time (min)	Yield[b] (%)
1	30	30	92
2	40	30	90

[a]Reaction conditions: isatoic anhydride (1 mmol), isatin (1 mmol), ZnO nanoparticles (10 mol %) in 5 mL THF under sonic condition with ultrasonic power 100 W at room temperature 30 °C. [b]Isolated yield.

Table 4 The comparison of catalytic efficiency of ZnO nanoparticles and bulk ZnO on the yield of indolo[2,1-*b*]quinazoline-6,12-dione under ultrasonication[a]

Entry	Catalyst	Reaction time (min)	Yield[b] (%)
1	ZnO nanoparticles (10 mol %)	30	92
2	Bulk ZnO	30	64

[a]Reaction conditions: isatoic anhydride (1 mmol), isatin (1 mmol), ZnO nanoparticles (10 mol %) in 5 mL THF under sonic condition with irradiation frequency 30 kHz and ultrasonic power 100 W at room temperature 30 °C. [b]Isolated yield.

Table 5 ZnO nanoparticles mediated synthesis of indolo[2,1-b]quinazoline-6,12-diones under ultrasonic irradiation[a]

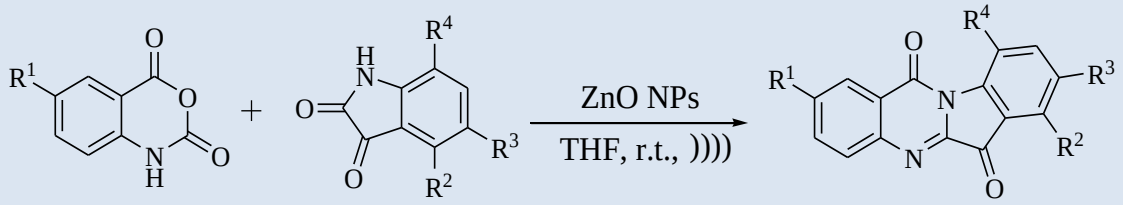

1(a-e) **2(a-j)** **3(a-v)**

Entry	R^1	R^2	R^3	R^4	Product	Reaction Time[b] (min)	Yield[c] (%)	M.P. (°C) [Ref.]
1	H	H	H	H	**3a**	30	92	272 [13]
2	H	H	OCH_3	H	**3b**	30	90	268 [13]
3	H	H	NO_2	H	**3c**	40	91	258 [12]
4	H	H	Cl	H	**3d**	35	92	294 [13]
5	H	H	Br	H	**3e**	35	91	292 [13]
6	H	H	F	H	**3f**	40	89	262 [12]
7	H	H	CH_3	H	**3g**	40	91	280 [13]
8	H	CH_3	H	H	**3h**	35	88	264 [20]
9	H	Cl	H	H	**3i**	30	89	291[20]
10	H	H	H	CH_3	**3j**	40	88	212 [20]
11	OCH_3	H	OCH_3	H	**3k**	30	90	281 [13]
12	OCH_3	H	CH_3	H	**3l**	35	89	292 [13]
13	CH_3	H	H	H	**3m**	30	92	254 [20]
14	CH_3	H	CH_3	H	**3n**	30	88	246 [20]
15	Br	H	CH_3	H	**3o**	3.0	92	>310 [13]
16	Br	H	NO_2	H	**3p**	45	89	298 [12]
17	Br	H	Br	H	**3q**	35	94	>310 [13]
18	Cl	H	OCH_3	H	**3r**	30	93	274 [12]
19	Cl	H	CH_3	H	**3s**	30	90	258 [12]
20	Cl	H	Cl	H	**3t**	30	93	290 [13]
21	CH_3	CH_3	H	H	**3u**	35	92	252[20]
22	CH_3	H	H	CH_3	**3v**	40	88	232[20]

[a]Reaction conditions: isatoic anhydride (1 mmol), isatin (1 mmol), ZnO nanoparticles (10 mol %) in 5 mL THF under sonic condition with irradiation frequency 30 kHz and ultrasonic power 100 W at room temperature 30 °C. [b]Reaction progress monitored by TLC. [c]Isolated yield.

To evaluate the scope and generality of the developed methodology, a series of indolo[2,1-*b*]quinazoline-6,12-diones were synthesized using ZnO nanoparticles in THF at room temperature under ultrasonication. The results in **Table 5** (Entries 1–22) clearly demonstrated that the protocol could be applied to various isatoic anhydrides and

isatins with quantitative yields. It is worth mentioning that the electronic nature of substituents on isatoic anhydrides and isatins has no distinct effect on product yield. The identity of all the products was ascertained on the basis of physical constant, FTIR, ^{1}H NMR, ^{13}C NMR and mass spectroscopy. The spectroscopic data is consistent with the proposed structures and in harmony with the literature values.

Recovery and reuse of the catalyst is a very important aspect of any chemical process for sustainability. Compared to the traditional catalysts, easy recycling is an attractive property of many metal oxide nanocatalysts. Consequently, we have investigated the catalytic activity of recycled ZnO nanoparticles for the synthesis of indolo[2,1-*b*]quinazoline-6,12-dione (**3a**). After completion of the reaction to separate the catalyst from the product, the solid product was dissolved in ethyl acetate and catalyst was separated by centrifugation. Then it was washed three to four times with 10 mL portions of ethyl acetate and dried at 150 °C for 5 h. The separated catalyst was then subjected to a new run of model reaction with fresh reactants. The comparison of efficiency of ZnO nanocatalyst in the model reaction for the synthesis of indolo[2,1-*b*]quinazoline-6,12-dione up to five consecutive cycles is shown in **Figure 4**. These results indicate that nanosized ZnO could be reused for at least four times with marginal reduction in the product yield.

The mechanism for the formation of indolo[2,1-*b*]quinazoline-6,12-dione (**3a**) is depicted in **Figure 5**. It is clear that the ultrasonic irradiation increases adsorption of isatoic anhydride on the surface of ZnO nanoparticles. In addition, ultrasonication can increases the mass transfer between isatoic anhydride and isatin via the acoustic cavitation effcet and assist in the breakdown of intermediates and desorption of products from the catalyst surface. In the present work, the role catalyst is the enhancemnet of electrophilic character of carbonyl carbon at position 2 of isatoic anhydride **1a** by lewis acidic Zn^{2+} sites. This leads to the nucleophilic attack by isatin **2a** at position 4 of isatoic anhydride resulting in formation of the intermediate **A** due to cleavage of the anhydride ring. The decarboxylation of formed intermediate **A** results in the formation of **B** which then undergoes intramolecular cyclization at position 2 of isatin and converted into final product **3a** with loss of water molecule.

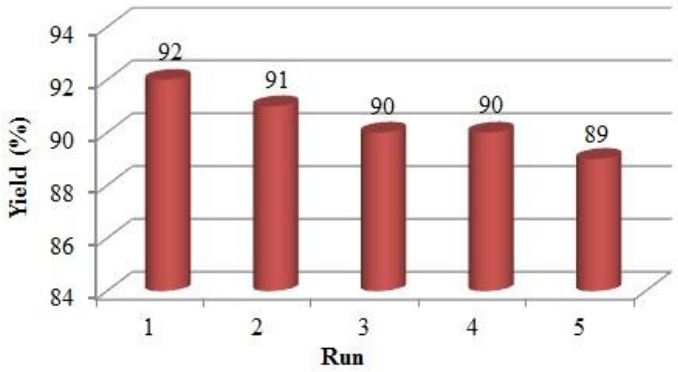

Figure 4 Reusability of ZnO nanoparticles for the synthesis of indolo[2,1-*b*]quinazoline-6,12-dione

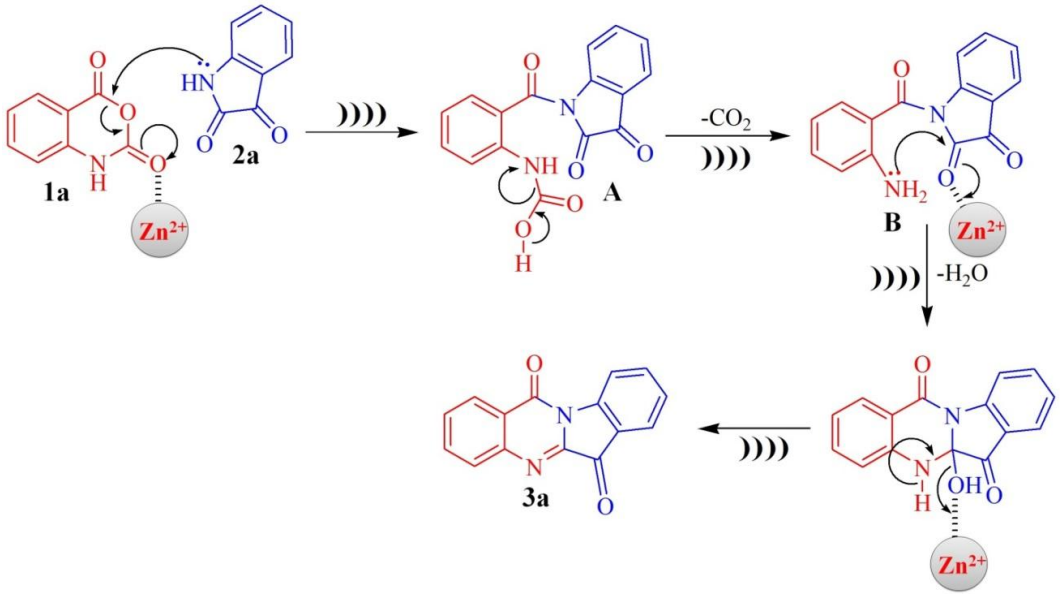

Figure 5: Plausible mechanism for the ZnO nanoparticles catalyzed synthesis of indolo[2,1-*b*]quinazoline-6,12-dione.

Conclusion

In summary, we offer an efficient and environmentally benign method to synthesize tryptanthrins using ZnO nanoparticles as a heterogeneous catalyst under ultrasound irradiation. The characteristic features of the catalyst include simple preparation, cost effectiveness, easy and rapid separation from reaction product, moisture insensitivity, reusability and ecofriendly nature which make the catalytic system superior in comparison with other metal based catalysts. The key features of present protocol such as simplicity, mild reaction conditions and high yields of desired products without side reactions are in good agreement with the green chemistry principles.

Acknowledgment

The authors acknowledge UGC for providing financial assistance under the scheme of Major Research Project 41-305/2012 (SR) for availing research facilities in Research Laboratory in Heterocyclic Chemistry at Devchand College, Arjunnagar, Maharashtra, India.

References

[1] J. P. Michael, Nat. Prod. Rep. 2007, 24, 223.
[2] A. Kamal, B. V. Subba Reddy, B. Sridevi, A. Ravikumar, A. Venkateswarlu, G. Sravanthi, J. Padma Sridevi, P. Yogeeswari, D. Sriram, Bioorg. Med. Chem. Lett. 2015, 25, 3867.
[3] R. Kaur, S. K. Manjal, R. K. Rawal, K. Kumar, Bioorg. Med. Chem. 2017, 25, 4533.
[4] F. Schindler, H. Zahner, Arch. Microbiol. 1971, 79, 187.
[5] K. Iwaki, E. Ohashi, N. Arai, K. Kohno, S. Ushio, M. Taniguchi, S. Fukuda, J. Ethnopharmacol. 2011, 134, 450.
[6] J. M. Hwang, T. Oh, T. Kaneko, A. M. Upton, S. G. Franzblau, Z. Ma, S. N. Cho, P. Kim, J. Nat. Prod. 2013, 76, 354.
[7] Y. Takei, T. Kunikata, M. Aga, S. Inoue, S. Ushio, K. Iwaki, M. Ikeda, M. Kurimoto, Biolog. Pharm. Bull. 2003, 26, 365.
[8] M. J Micallef, K. Iwaki, T. Ishihara, S. Ushio, M. Aga, T. Kunikata, S. Koya-Miyata, T. Kimato, M. Ikeda, M. Kurimoto, Int. Immunopharmacol. 2002, 2, 565.
[9] J. Scovill, E. Blank, M. Konnick, E. Nenortas, T. Shapiro, Antimicrob. Agents Chemother. 2002, 46, 882.
[10] D. V. Gruznev, D. N. Chubenko, A. V. Zotov, A. A. Saranin, J. Phys. Chem. C 2010, 114, 14489.
[11] M. J. Novak, J. C. Baum, J. W. Buhrow, J. A. Olson, Surf. Sci. 2006, 600, L269.
[12] A. Kumar, V. D. Tripathi, P. Kumar, Green Chem. 2011, 13, 51.
[13] M. El-Remaily, O. M. Elhady, Tetrahedron Lett. 2016, 57, 435.
[14] T. V. Moskovkina, A. I. Kalinovskii, V. V. Makhan'kov, Russ. J. Org. Chem. 2012, 48, 123.
[15] B. Batanero, F. Barba, Tetrahedron Lett. 2006, 47, 8201.
[16] J. L. Liang, S. -E. Park, Y. Kwon, Y. Jahng, Bioorg. Med. Chem. 2012, 20, 4962.
[17] F. -C. Jia, Z. -W. Zhou, C. Xu, Y. -D. Wu, A. -X. Wu, Org. Lett. 2016, 18, 2942.
[18] G. -J. Mei, C. -Y. Bian, G. -H. Li, S. -L. Xu, W. -Q. Zheng, F. Shi, Org. Lett. 2017, 19, 3219.
[19] T. V. Moskovkina, M. V. Denisenko, A. I. Kalinovskii, V. A. Stonik, Russ. J. Org. Chem. 2013, 49, 1740.
[20] C. Wang, L. Zhang, A. Ren, P. Lu, Y. Wang, Org. Lett. 2013, 15, 2982.
[21] T. Abe, T. Itoh, T. Choshi, S. Hibino, M. Ishikura, Tetrahedron Lett. 2014, 55, 5268.
[22] A. C. Nelson, E. S. Kalinowski, T. L. Jacobson, P. Grundt, Tetrahedron Lett. 2013, 54, 6804.
[23] A. V. Lygin, A. de Meijere, Org. Lett. 2009, 11, 389.
[24] Z. -J. Cai, S. -Y. Wang, S. -J. Ji, Org. Lett. 2013, 15, 5226.
[25] S. D. Vaidya, N. P. Argade, Org. Lett. 2013, 15, 4006.
[26] B. V. Subba Reddy, D. Maheswara Reddy, G. Niranjan Reddy, M. Ramana Reddy, V. Krishna Reddy, Eur. J. Org. Chem. 2015, 2015, 8018.
[27] S. Guo, Y. Li, L. Tao, W. Zhang, X. Fan, RSC Adv. 2014, 4, 59289.
[28] C. Zhang, S. Li, F. Bures, R. Lee, X. Ye, Z. Jiang, ACS Catal. 2016, 6, 6853.
[29] X. Li, H. Huang, C. Yu, Y. Zhang, H. Li, W. Wang, Org. Lett. 2016, 18, 5744.
[30] H. Hou, H. Li, Y. Han, C. Yan, Org. Chem. Front. 2018, 5, 51.
[31] J. Zhang, W. Yu, L. Zhang, Phys. Lett. 2002, 299, 276.
[32] Q. Zhang, C. Xie, S. Zhang, A. Wang, B. Zhu, L. Wang, Z. Yang, Sens. Actuator B-Chem. 2005, 110, 370.
[33] A. C. Pandey, S. S. Sanjay, R. S. Yadav, J. Exp. Nanosci. 2010, 5, 488.
[34] J. Safaei-Ghomi, M. A. Ghasemzadeh, Arab. J. Chem. 2017, 10, S1774.

[35] S. Swami, N. Devi, A. Agarwala, V. Singh, R. Shrivastava, Tetrahedron Lett. 2016, 57, 1346.
[36] J. Kothandapani, A. Ganesan, G. Kumar Mani, A. J. Kulandaisamy, J. B. B. Rayappan, S. S. Ganesan, Tetrahedron Lett. 2016, 57, 3472.
[37] S. Sadjadi, M. Eskandari, Ultrason. Sonochem. 2013, 20, 640.
[38] H. Naeimi, A. Didar, Ultrason. Sonochem. 2017, 34, 889.
[39] J. Kaur Rajput, P. Arora, G. Kaur, M. Kaur, Ultrason. Sonochem. 2015, 26, 229.
[40] J. Safari, L. Javadian, Ultrason. Sonochem. 2015, 22, 341.
[41] A. Javidan, A. Ziarati, J. Safaei-Ghomi, Ultrason. Sonochem. 2014, 21, 1150.
[42] A. A. Oladiran, I. A. M. Olabisi, Can. J. Pure Appl. Sci. 2013, 7, 2635.
[43] G. K. Mani, J. B. B. Rayappan, Sens. Actuators B-Chem. 2016, 223, 343.
[44] J. R. Reddy, G. K. Mani, P. Shankar, J. B. B. Rayappan, Sens. Lett. 2014, 12, 1451.

Publication History
Received 14th May 2018
Revised 18th June 2018
Accepted 04th July 2018
Online 30th July 2018